

## Corrosion Passivation in Aerated 3.5% NaCl solutions of Brass by Nanofiber Coatings of Polyvinyl Chloride and Polystyrene

Mahir Es-saheb<sup>1</sup>, El-Sayed M. Sherif<sup>2,3,\*</sup>, Ahmed El-Zatahry<sup>4,5</sup>, Magdy M. El Rayes<sup>1,#</sup>, Khalil Abdelrazek Khalil<sup>1</sup>

<sup>1</sup> Mechanical Engineering Department, King Saud University, P.D. Box 800, Riyadh 11421, Saudi Arabia

<sup>2</sup> Center of Excellence for Research in Engineering Materials (CEREM), Advanced Manufacturing Institute, King Saud University, P. O. Box 800, Riyadh 11421, Saudi Arabia

<sup>3</sup> Electrochemistry and Corrosion Laboratory, Department of Physical Chemistry, National Research Centre (NRC), Dokki, 12622 Cairo, Egypt

<sup>4</sup> Petrochemical Research Chair, Chemistry Department, College of Science, King Saud University, B.O. Box 2455 Riyadh 11451, Saudi Arabia

<sup>5</sup> Advanced Technology and New Materials Research Institute, City of Scientific Research and Technology Applications, New Boarg El-Arab City, Alexandria, Egypt.

# On leave from Production Engineering Department, Faculty of Engineering, Alexandria University, Egypt.

\* E-mail: [esherif@ksu.edu.sa](mailto:esherif@ksu.edu.sa); [emsherif@gmail.com](mailto:emsherif@gmail.com), Fax: 096614670199

Received: 26 September 2012 / Accepted: 13 October 2012 / Published: 1 November 2012

---

Nanocomposite coatings exhibit superior properties including corrosion and wear resistances compared to the plain non-composite ones. In this work, the deposition of polyvinyl chloride (PVC) and polystyrene (PS) nanofiber coatings on brass surface was carried out. The work was also extended to study the effects of PVC and PS on the corrosion passivation of brass in aerated 3.5 wt.% sodium chloride (NaCl) solutions. The PVC and PS coatings were prepared and deposited on brass surface using electrospinning technique. The nanofibers coating layers were characterized using optical (OM) and scanning electron (SEM) microscopes. The OM and SEM micrographs depicted that the PVC and PS coatings consist of dense and compact entangled nanofibers that completely cover up the brass surface. The corrosion measurements were performed by cyclic potentiodynamic polarization (CPP) and electrochemical impedance spectroscopy (EIS) techniques on the uncoated and PVC and PS coated brass surfaces in NaCl solutions. Both CPP and EIS data confirmed that PVC and PS coatings protect the brass surface from being corroded through minimizing its corrosion current and corrosion rate and increasing its polarization resistance.

---

**Keywords:** brass corrosion; corrosion passivation, electrospinning; nanofiber coatings; polystyrene; polyvinyl chloride

## 1. INTRODUCTION

Brass materials are relatively noble for which brass possesses attractive properties, namely, good corrosion resistance, good machinability, high thermal and electrical conductivity and better resistance to biofouling. It has been widely used in water distribution systems, water treatment units, condensers, desalination, power plant condensers and petrochemical heat exchangers, shipboard condensers, and many other applications [1-8]. Brass with 65% Cu and 35% Zn is prone to corrosion attack when exposed to a corrosive media because of the brass  $\alpha$ -phase. Increasing the zinc content in the alloy changes the  $\alpha$ -phase to  $\beta$ -phase and accelerates corrosion damage [1]. Dezincification of brass is one of the well-known and common processes by means of which brass loses its valuable physical and mechanical properties leading to failure of structure [1,9-13]. Therefore, the corrosion mechanism and corrosion prevention of brass in different corrosive media has been attracted many investigators [10-15].

One of the most important methods and is considered as the first line defense in the protection of metal and alloy structures against corrosion in harsh environments is the use of protective coatings. Coatings impart specific engineering properties of a substrate material by modifying or applying a thin layer at its surface and there have been trials to develop nano-protective coatings [16-19]. A nanocoating is a coating that comprises of at least one constituent with dimensions in nano-scale. Small particle size (nanoscale) imparts nanocoating with a large number of surface atoms, high surface energy, spatial confinement and reduced imperfections resulting in improved physical, mechanical, chemical and optoelectronic properties. Due to this reason, there is considerable interest among researchers to use nanomaterials for a range of products including nanocoatings [20,21] with improved strength, hardness, corrosion behavior and/or increased wear, friction, abrasion, and scratch resistance.

Due to the large number of possible combinations between coating materials and the substrate, a wide variety of technological applications can be met by nanocomposite coatings [22]. The preparation of these coatings has been produced using different methods such as electrospinning, phase's separation, self-assembly, drawing, and template synthesis [23-27]. Electrospinning technique produces nano-woven fibrous structures of polymer coatings with fiber diameters ranging from tens of nanometers to microns deposited on the surface of materials. At these conditions, the materials earn excellent properties like large surface area to volume ratio, flexibility in surface functionalities, and superior mechanical performance [17-20]. In some cases, the nanofiber coatings enhance reliability and performance of various structural components to enable them to resist corrosion, pitting, exfoliation, erosion, sliding and wear. Corrosion and wear resistant coatings can be used in a variety of industries such as in automobile, power generation, utility, aerospace, defense, optical equipment, magnetic storage devices and bearings, engine parts and seals, etc [20,21,28-32]. These outstanding properties make the polymer nanofibers to be optimal candidates for many important applications.

We have been studying the deposition of polymer coating nanofibers on metallic substrates and reporting their corrosion behavior in corrosive media [33,34]. In this work, we report the fabrication of polyvinyl chloride (PVC) and polystyrene (PS) nanofiber coatings, then their deposition on a brass substrate by using the electrospinning of the PVC and PS polymer solutions. The effects of PVC and PS on the corrosion protection of brass (65 wt.% Cu / 35 wt.% Zn) in 3.5% NaCl solutions were also

examined using cyclic polarization, electrochemical impedance spectroscopy and scanning electron microscope investigations.

## 2. EXPERIMENTAL PROCEDURES

### 2.1. Electrospinning deposition of polymer coatings

The electrospinning process was carried out using separated solutions of PVC and PS polymers. The PS solution in a concentration of 10 wt. % was prepared by adding appropriate amount of PS into tetrahydrofuran (THF) and stirring over the whole night at room temperature. This solution was used for electrospinning under the following conditions; 70 KV applied voltage, 4 round per minute (rpm) rotating speed of electrospinning electrode, 14 cm the distance of the collecting electrode and collector, and 70 % was the ambient humidity. The PVC solution in a concentration of 12 wt. % was prepared by dissolving the polymer in a THF solvent at 30°C and stirring overnight to be used for electrospinning the nanofiber on brass sheet surfaces. The electrospinning conditions were of 80 KV, the distance between the electrode and collector was 18 cm, and range of the speed of rotating electrode was from 4 to 5 rpm.

### 2.2. Electrospinning setup

The polymer solutions were electrospun using needleless laboratory machine called a nano spider laboratory (NSLAB 500S), which is represented by the image shown in Fig 1. The NSLAB 500S consists of spinning head tub where rotating spinning electrode is wetted in solution under high voltage.



**Figure 1.** The nano spider laboratory (NSLAB) 500S instrument.

Nanofibers are coating exchangeable substrate belt which is moving along the static collecting electrode. Internal control parameters of the process are electrode distance, high voltage, electrode speed and substrate speed. External parameters used for control of electrospinning throughput and nanofiber quality are solution characteristics (viscosity, conductivity) and air properties (temperature, relative humidity). The prepared PVC and PS solutions were electrospun at 15-kV positive voltage, 15-cm working distance, and 0.3-mL/h solution flow rate. The electrospun nanofibers were collected on brass (65 wt.% Cu / 35 wt.% Zn) surfaces, air dried in a hood at room temperature for overnight, then quickly rinsed in distilled water, and finally dried under vacuum oven at room temperature overnight. The schematic representation on how the nanofiber coatings were applied onto the surfaces of the tested substrates is shown in Fig. 2.

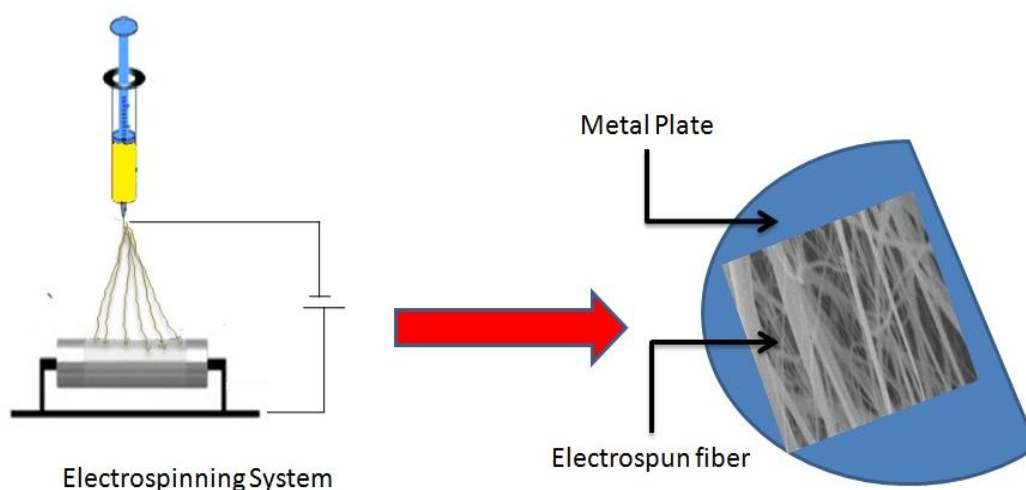


**Figure 2.** A schematic representation shows the production of the PVA and PVC nanofiber coatings.

### 2.3. Nanofibers morphological characterization

Surface morphology of electrospun nanofibers on the brass surface were investigated using scanning electron microscopy (JSM-7100F). After sputter coating with Gold, the fiber size distribution was measured up to five frames of randomly selected SEM micrograph using software. The thickness of electrospun mats and films was measured using PRECISION MICROMETER, Model No. 49-61, Range 0-1.270 mm, Testing Machines INC. AMITVILLE N.Y. (USA).

### 2.4. Electrochemical corrosion measurements

The uncoated and PVC and PS coated brass for corrosion measurements were prepared by attaching an insulated copper wire to one face of the sample using an aluminum conducting tape, and then isolated by cold mounted in resin before letting it to dry in air for 24 h at room temperature. To prevent the possibility of crevice corrosion during measurement, the interface between sample and resin was coated with Bostik Quickset, a polyacrylate resin. The area of the other face of the samples,

on which the measurements was carried out, was 1.0 cm<sup>2</sup>. The test solution, 3.5 wt.% NaCl, was prepared by dissolving 35 g of NaCl in 1 L glass flask.

Electrochemical measurements were carried out by using a PARC Parstat-2273 Advanced Electrochemical System after immersing the uncoated and coated electrodes for 20 minutes in freely aerated stagnant 3.5 wt.% NaCl solutions. The cyclic potentiodynamic polarization (CPP) curves were obtained by sweeping the potential from -1200 mV in the positive direction up to 500 mV vs. Ag/AgCl at a scan rate of 1 mV/s. The potential was also swept in the backward direction with the same scan rate from 500 mV towards the more negative direction, in order to see whether pitting corrosion of brass occurs. Electrochemical impedance spectroscopy (EIS) experiments were collected at the open-circuit potential of brass by scanning the frequency from 100 kHz to 0.1 Hz with an ac wave of  $\pm 5$  mV peak-to-peak overlaid on a dc bias potential, and the Nyquist plots were acquired using Powersine software at a rate of 10 points per decade change in frequency.

### 3. RESULTS AND DISCUSSION

#### 3.1. Optical (OM) and scanning electron microscopy (SEM) investigations

The optical micrographs for (a) uncoated brass, (b) PVC coated brass and (c) PS coated brass surfaces are shown respectively in Fig. 3. It is clearly seen from Fig. 3 that, the PVC and PS coating layers fully covered the brass surface, which could led to the change of surface morphology and color seen for image (b) and image (c) of Fig. 3. These layers look also compact and homogeneously distributed on the brass surface.

In order to report the morphology of the coated PVC and PS films on the brass surface, scanning electron microscopy (SEM) investigations were carried out and the images are shown respectively in Fig. 4 and Fig. 5. A typical SEM micrograph, Fig.4a, exhibits a web of randomly oriented PVC fibers on a large area the brass surface. A high magnification SEM image as shown in Fig. 4b, also exhibits a web of randomly oriented fiber with a broad distribution from 205 to 250 nm. As well as, the SEM images for PS/brass shown in Fig. 5 (a) and Fig. 5 (b) indicate that the PS fiber layers are denser and compact on the brass surface. The PS fibers were also oriented and distributed randomly with a broad thickness from 1.05  $\mu\text{m}$  to 1.8  $\mu\text{m}$ .

For more confirmation on the thickness of the coated PVC and PS layers on the brass surface, the SEM side view images were taken as shown in Fig. 6a and Fig. 6b, respectively. The coated PVC film on the brass surface as depicted in Fig. 6a recorded an average thickness size of about 6.0  $\mu\text{m}$ . This is because the PVC layer is compact and dense enough to homogeneously cover up the brass surface. As well as, the PS coated layer and represented in Fig. 6b proves that the PS coating is also uniformly distributed, compact, and dense on the brass surface and the thickness of the electrospun deposited film vary from 10 to 14  $\mu\text{m}$ .

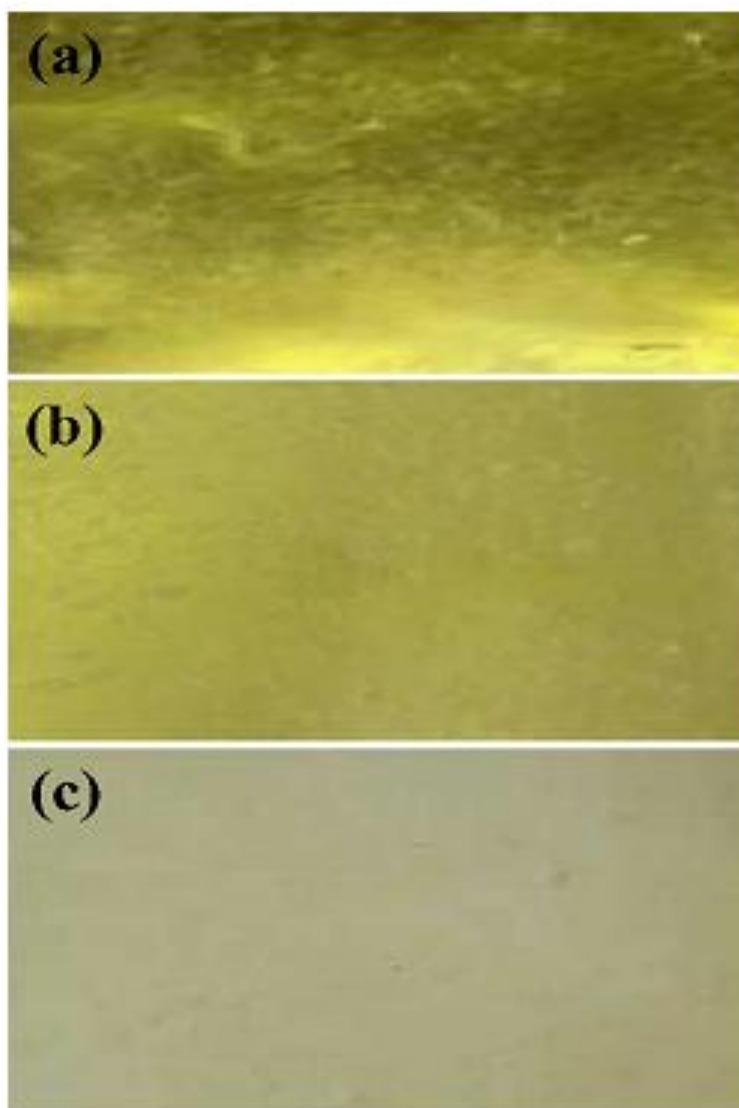


**Figure 3.** The Optical microscopy images for (a) uncoated brass, (b) PVC coated brass and (c) PS coated brass surfaces, respectively.

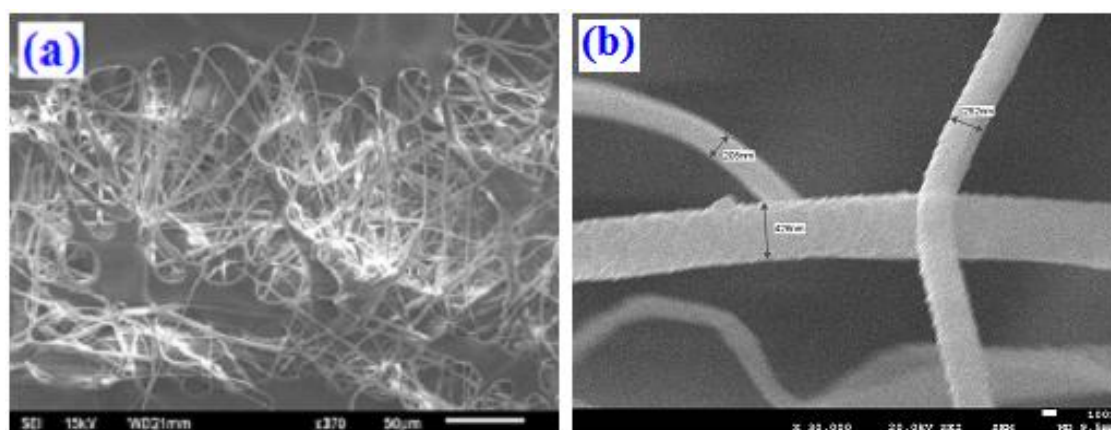


**Figure 4.** SEM micrographs for the coated PVC on the brass surface; (a) a large area of the surface and (b) a high magnification image shows a small area of the surface.

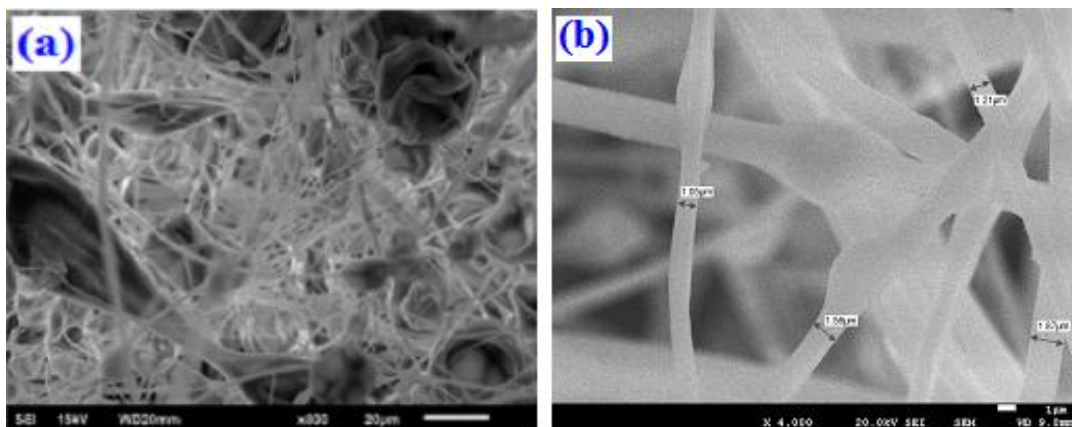


Figure 5. SEM micrographs for the polystyrene coating deposited on the brass surface; (a) a large area of the surface and (b) a high magnification image shows a small area of the surface.

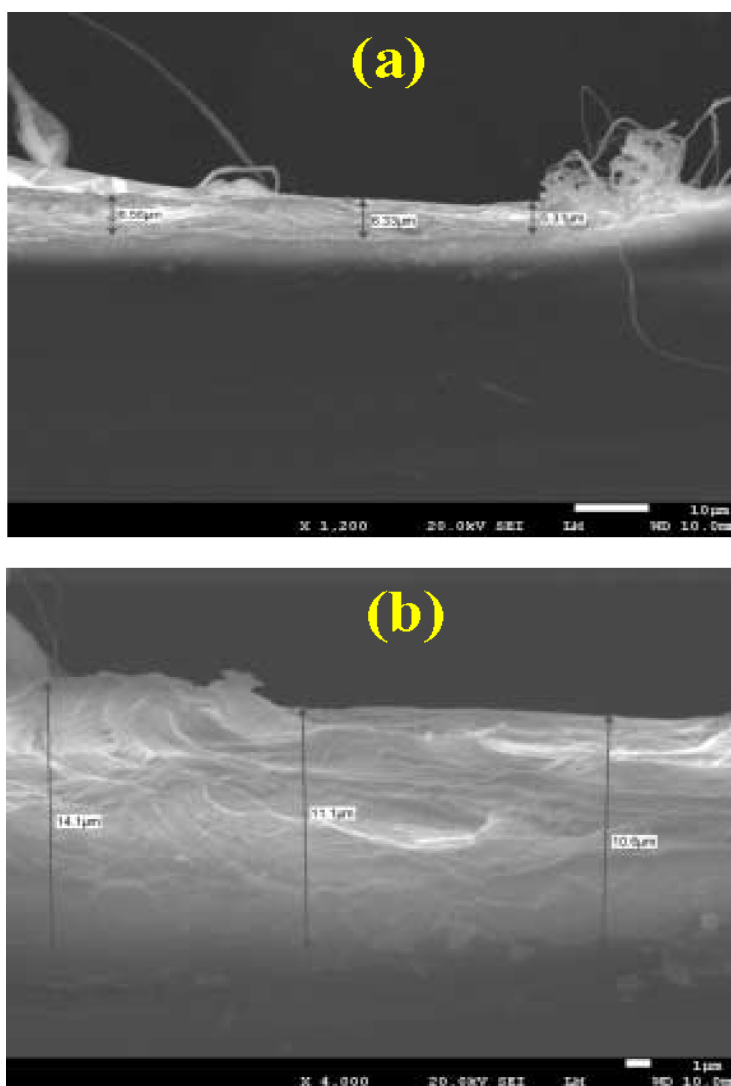


Figure 6. Scanning electron microscopy (SEM) images for (a) PVC and (b) PS electrospun fiber films over brass substrate (Side View).

3.2. Cyclic potentiodynamic polarization (CPP) curves

The CPP curves obtained for (a) bare brass, (b) PVC coated brass, and (c) PS coated brass electrodes after their immersion for 20 min in freely aerated 3.5 wt.% NaCl solution are shown respectively in Fig. 7. The corrosion parameters, the corrosion potential ( $E_{Corr}$ ), corrosion current ( $j_{Corr}$ ), cathodic ( $\beta_c$ ) and anodic ( $\beta_a$ ) Tafel slopes, polarization resistance ( $R_p$ ), and corrosion rate ( $K_{Corr}$ ), obtained from the polarization data are presented in Table 1. The  $j_{Corr}$  and  $E_{Corr}$  parameters were obtained from the extrapolation of anodic and cathodic Tafel lines located next to the linearized current regions [35-40]. The values of  $R_p$  and  $K_{Corr}$  were calculated from the polarization curves according to the following equations [39,40]:

$$R_p = \frac{1}{j_{Corr}} \left( \frac{\beta_c \cdot \beta_a}{2.3(\beta_c + \beta_a)} \right) \tag{1}$$

$$K_{Corr} = \frac{j_{Corr} k E_w}{d A} \tag{2}$$

Where,  $k$  is a constant that defines the units for the corrosion rate ( $= 3272 \text{ mm/ (amp. cm. year)}$ ),  $E_w$  the equivalent weight in grams/equivalent of the brass ( $E_w = 32.1 \text{ grams/equivalent}$ ),  $d$  the density in  $\text{g cm}^{-3}$  ( $d = 8.32 \text{ g/cm}^3$ ), and at the area of the exposed surface of the electrode in  $\text{cm}^2$  ( $A = 1 \text{ cm}^2$ ).

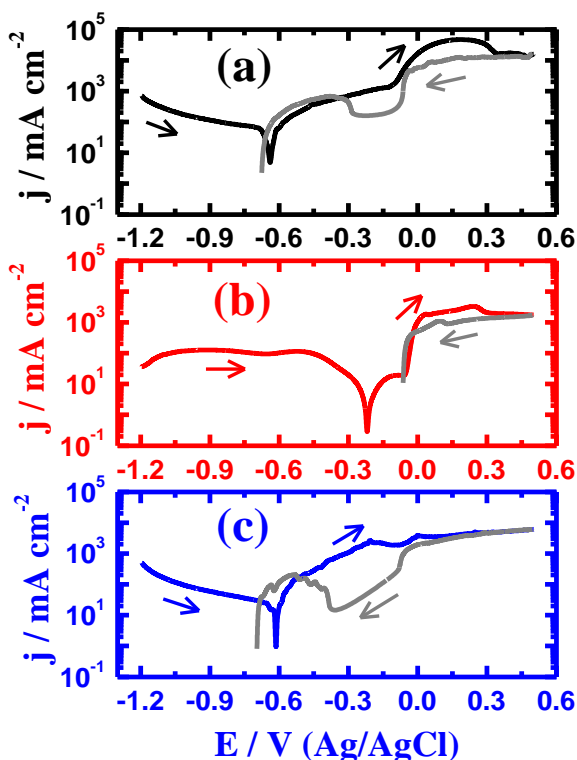
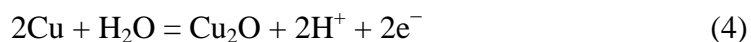


**Figure 7.** Cyclic potentiodynamic polarization curves obtained for (a) bare brass, (b) brass coated with PVC, and (c) brass coated with PS electrodes after their immersion for 20 min in 3.5 wt.% NaCl solution.

The cathodic reaction for metals and alloys in aerated neutral solutions has been reported to be the oxygen reduction as follows [41,42],



According to Karpagavalli and Rajeswari [43], when brass electrode is exposed to a saline electrolyte, its anodic reactions will take place according to the following reactions,



This means that the corrosion of the uncoated brass occurs mainly due to the dissolution of Zn, in addition the presence of high concentration of chloride ions, 3.5 wt.% also increases the corrosion of brass by dissolving the formed copper oxide on the surface of the alloy [43]. For the PVC and PS coated brass surfaces, these reactions (Eq. 4 and Eq. 5) seem to be less likely to occur due to the presence of the homogenous layers of PVC and PS coatings. This is confirmed by the values of the corrosion parameters listed in Table 1. Where, the corrosion current for brass in the presence of the polymer coatings was reduced from 78  $\mu\text{A} / \text{cm}^2$  for uncoated brass to only 8.5  $\mu\text{A} / \text{cm}^2$  for PVC coated brass and 22  $\mu\text{A} / \text{cm}^2$  for PS coated surface. This effect also increased the values of polarization resistance,  $R_p$ , and decreased the values of corrosion rate,  $K_{\text{Corr}}$ . The obtained polarization data thus proved that the presence of PVC and PS nanofiber coatings on the brass surface eliminates the corrosion of brass in 3.5 wt.% NaCl solutions and effect increases in the order PVC > PS.

**Table 1.** Corrosion parameters obtained from polarization curves shown in Fig. 7 for uncoated and PVC and PS coated brass electrodes after their immersion in 3.5% NaCl solutions for 20 min before measurement.

Material	Parameter					
	$-\beta_c / \text{Vdec}^{-1}$	$E_{\text{Corr}} / \text{V}$	$j_{\text{Corr}} / \mu\text{Acm}^{-2}$	$\beta_a / \text{Vdec}^{-1}$	$R_p / \text{k}\Omega \text{cm}^2$	$K_{\text{Corr}} / \text{mmy}^{-1}$
Uncoated Brass	0.30	-0.670	78	0.21	0.69	0.985
PVC coated Brass	0.15	-0.225	8.5	0.21	4.46	0.107
PS coated Brass	0.23	-0.632	22	0.235	2.30	0.278

### 3.3. Electrochemical impedance spectroscopy (EIS) measurements

In order to shed more light on the effect of PVC and PS nanofiber coatings on the protection of brass surface from being corroded and to determine kinetic parameters for electron transfer reactions at the brass/electrolyte and brass-coating/electrolyte interface, the EIS investigations were carried out. We have been successfully using the EIS technique to study the corrosion and corrosion inhibition of

metals and alloys at similar conditions [44-49]. Fig. 8 shows the typical Nyquist impedance plots obtained at an open-circuit potential value for (a) uncoated brass, (b) PVC coated brass and (c) PS coated brass electrodes, respectively after 20 min of their immersion in 3.5 wt.% NaCl solutions. The EIS plots were also analysed by best fitting to an equivalent circuit model as shown in Fig. 9. The impedance parameters obtained from the equivalent circuit are recorded in Table 2.

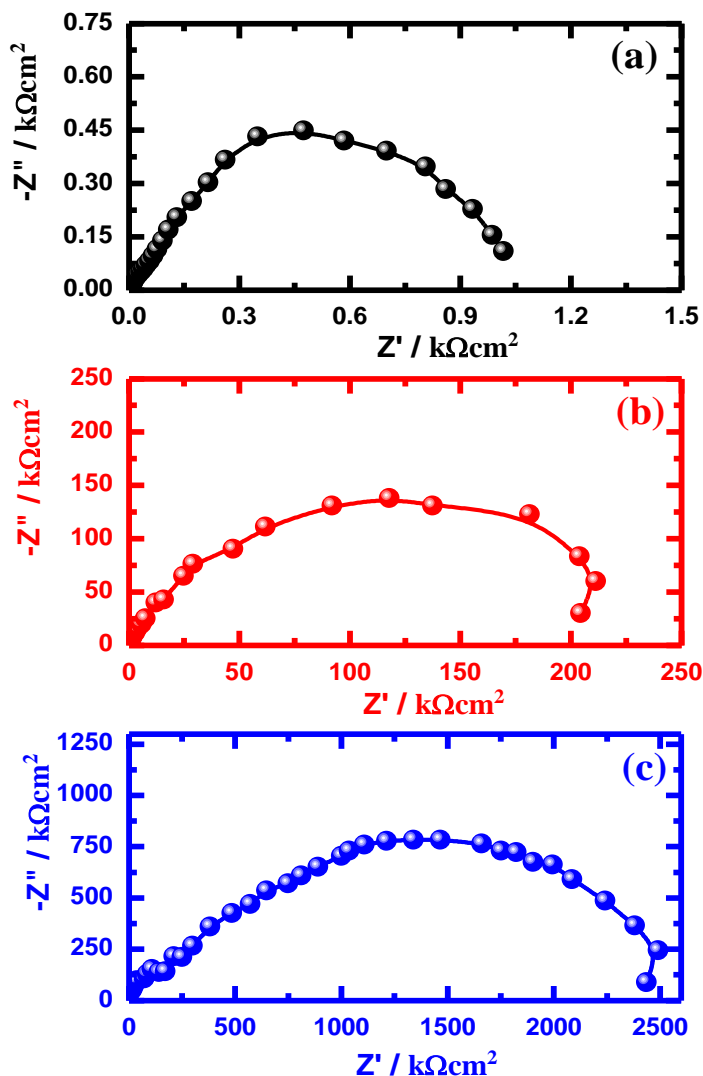


**Figure 8.** EIS Nyquist plots obtained for (a) bare brass, (b) brass coated with PVC, and (c) brass coated with polystyrene electrodes after their immersion for 20 min in freely aerated 3.5 wt.% NaCl solutions.

It is clearly seen from Fig. 8a that the brass electrode shows only a single distorted semicircle. The diameter of this semicircle widely increased with the presence of PVC, Fig. 8b as well as PS nanofiber coating on the brass surface. This indicates that the surface gets more protected against corrosion in the chloride solution by coating it with electrospun PVC and PS nanofibers. According to Ma et. al (50), the semicircles at high frequencies are generally associated with the relaxation of

electrical double layer capacitors due to the decrease of brass corrosion by stabilizing the formed oxide film,  $\text{Cu}_2\text{O}$ , Eq. (4), on its surface and the decrease of the corrosivity of the chloride ions. Here, the diameters of the high frequency semicircles are usually considered as the charge transfer resistance, which increase in case of PVC and PS coated brass surfaces.

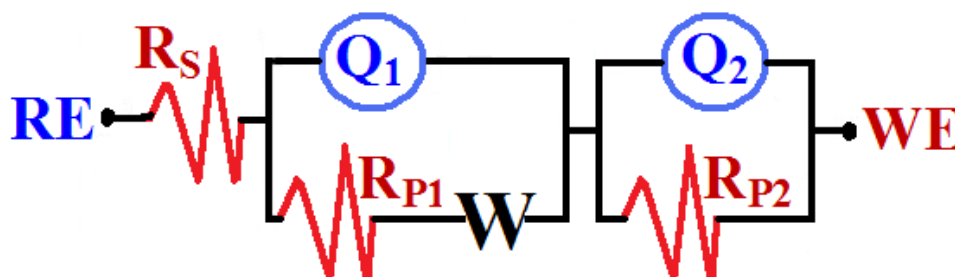


**Figure 9.** Equivalent circuit model used to fit the Nyquist plots presented in Fig. 8.

The EIS parameters of the circuit shown in Fig. 9 and listed in Table 2 can be defined as follows;  $R_S$  represents the solution resistance between aluminum electrodes and the counter (platinum) electrode,  $Q_1$  and  $Q_2$  the constant phase elements (CPEs),  $R_{P1}$  the resistance of a film layer formed on the surface of aluminum,  $R_{P2}$  accounts for the polarization resistance at the aluminum surface, and  $W$  the Warburg impedance. Table 2 shows that the values of  $R_S$ ,  $R_{P1}$  and  $R_{P2}$  recorded higher values for the PVC and PS coated brass surfaces. The CPEs,  $Q_1$  with its  $n$  value exactly 1.0 represent double layer capacitors. The CPEs,  $Q_2$  with its  $n$  value is almost 1.0 represent another double layer capacitors with some pores; the CPEs decrease, while their  $n$ -values increase with the case of PVC and further with PS coated surface. The decrease of both  $Q_1$  and  $Q_2$  values in the presence of PVC and PS indicates that the coated brass surface is more protected against corrosion compared to the uncoated brass. The presence of the Warburg impedance ( $W$ ) gives another confirmation that the brass surface is well protected and its corrosion in the chloride solutions via mass transport is very unlikely to occur in the case of PVC and PS nanofiber coatings.

**Table 2.** Impedance parameters obtained by fitting the Nyquist plots shown in Fig. 7 with the equivalent circuit shown in Fig. 8 for brass electrodes after their immersion in 3.5 wt.% NaCl solutions for 20 min before measurements.

Material	Parameter							
	$R_S / \Omega \text{ cm}^2$	$Q_1$		$R_{P1} / \Omega \text{ cm}^2$	$W \Omega \text{ S}^{-1/2}$	$Q_2$		$R_{P2} / \Omega \text{ cm}^2$
		$Y_{Q1} / \mu\text{F cm}^{-2}$	$n$			$Y_{Q2} / \mu\text{F cm}^{-2}$	$n$	
Uncoated brass	3.7	20.53	1.00	40.60	$16.1 \times 10^{-8}$	0.156	0.87	995
PVC coated brass	12.4	0.384	1.00	4681	$4.14 \times 10^{-5}$	0.048	0.92	232600
PS coated brass	15.1	0.050	1.00	14900	$3.99 \times 10^{-7}$	0.009	0.95	905300

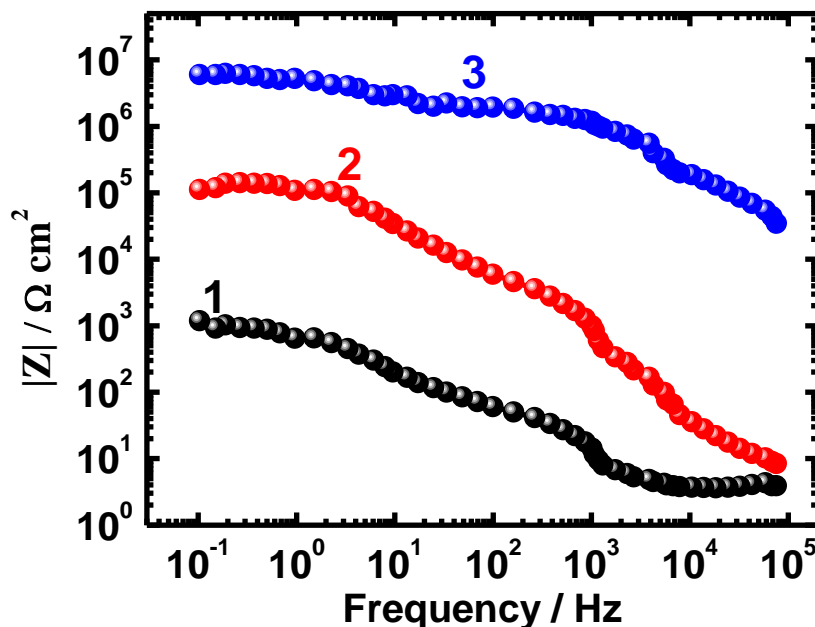


**Figure 10.** Typical impedance Bode plots obtained for (1) uncoated brass, (2) PVC coated brass, and (3) PS coated brass electrodes after their immersion for 20 min in freely aerated 3.5 wt.% NaCl solutions.

The data obtained from Nyquist plots were also confirmed by plotting the values of impedance ( $|Z|$ ) against frequency for (a) uncoated brass, (b) PVC coated brass, and (c) PS coated brass as presented by the Bode plots shown in Fig. 10. The lowest impedance values were recorded for the bare brass in the chloride solution, Fig. 10a. In the presence of PVC coating, Fig. 10b, brass recorded higher impedance values over the whole frequency range of the experiment. Further increments were obtained for the PS coated brass, Fig. 10c. According to Mansfeld et. al [51] the higher the impedance at low frequency values the higher the passivation of the surface against corrosion. The EIS data thus agree with the polarization data and both proved that PVC and PS nanofiber coatings provide enough protection for brass surface against corrosion in 3.5 wt.% NaCl solutions.

#### 4. CONCLUSION

The passivation of brass corrosion in aerated stagnant 3.5% NaCl solutions by polyvinyl chloride (PVC) and polystyrene (PS) nanofiber coatings has been investigated. The deposition of PVC and PS layers on the brass surface was applied by using electrospinning technology. The optical (OM) and scanning electron (SEM) microscopes were employed to characterize the layer of the nanofiber coatings. It was found that the coating layers of PVC and PS are homogeneously distributed on the brass surface with an average thickness of about 6.0  $\mu\text{m}$  for PVC and 10.0 ~ 14  $\mu\text{m}$  for PS. The effects of PVC and PS as protective coatings for brass against corrosion in 3.5 wt.% NaCl solutions were evaluated by cyclic potentiodynamic polarization (CPP) and electrochemical impedance spectroscopy

(EIS) techniques on the uncoated and PVC and PS coated brass surfaces in NaCl solutions. It has been found that the presence of PVC and PS on the brass surface decreases its corrosion in the test solution. The PVC and PS coatings decreased the corrosion current and corrosion rate of brass by decreasing its anodic and cathodic reactions as reported by the CPP data. This effect also increased the surface and polarization resistances for brass as was achieved by the EIS measurements. The combined results indicate that PVC and PS can be deposited on the brass surface and can be used as good protective coatings against corrosion in 3.5 wt.% NaCl solutions.

#### ACKNOWLEDGEMENTS

This work was financially supported by the National Plan for Science & Technology (NPST), King Saud University. Project No. 10-ADV1033-02.

#### References

1. R. Ravichandran, N. Rajendran, *Appl. Surf. Sci.*, 239 (2005) 182.
2. H.M. Shalaby, A. Al-Hashem, M. Lowther, J. Al-Besharah (Eds.), 'Industrial Corrosion and Corrosion Control Technology', Kuwait Institute for Scientific Research, Kuwait, 1996.
3. H.C. Shih, R.J. Tzou, *J. Electrochem. Soc.*, 138 (1991) 958.
4. M.I. Abbas, *Brit. Corros. J.*, 26 (1991) 273.
5. G. Quartarone, G. Moretti, T. Bellami, *Corrosion*, 54 (1998) 606.
6. Satendra Kumar, T.S.N. Sankara Narayanan, M. Suresh Kumar, A. Manimaran, *Int. J. Electrochem. Sci.*, 1 (2006) 456.
7. F. Mansfeld, T. Smith, *Corrosion*, 29 (1973) 3.
8. A. Weisstuch, K.R. Lange, *Mater. Protect. Perform*, 10 (1971) 29.
9. A.K. Mitra, *R&D J. NTPC*, 2 (1996) 52.
10. F. Mansfeld, T. Smith, P. Parry, *Corrosion*, 27 (1971) 289.
11. M. Ohsawa, W. Suetaka, *Corros. Sci.*, 19 (1979) 709.
12. S. Selvaraj, S. Ponmariappan, M. Natesan, N. Palaniswamy, *Corros. Rev.*, 21 (2003) 41.
13. N.W. Polan, in 'Metals Handbook, Corrosion, Vol. 13, ASM International, Materials Park, OH, 9th Edition, 1987.
14. A.G. Gad-Allah, M.M. Abou-Romia, M.W. Badawy, H.H. Rehan, *J. Appl. Electrochem.*, 21 (1991) 829.
15. D.A. Jones, 'Principles and Prevention of Corrosion', 2nd Edition, Prentice-Hall, Englewood Cliffs, NJ, 1996, p. 20.
16. Zheng-Ming Huang, Y.-Z. Zhang, M. Kotakic, S. Ramakrishna, *Compos. Sci. Technol.*, 63 (2003) 2223.
17. D. Luck, A. Sarkar, L. Martinov, K. Vodsed Ikov, D. Lubasov, J. Chaloupec, P. Pokorn, P. Mike, J. Chvojka, M. Komrek, *Journal Textile Progress*, 41(2009) 559.
18. Feng-Lei Zhou, Rong-hua Gong, Isaac Porat, *Polymer International*, 58 (2009) 331.
19. J.M. Deitzel, J. Kleinmeyer, J.K. Hirvonen, T.N.C. Beck, *Polymer*, 42 (2001) 8163.
20. F. Vaz, L. Rebouta, *Mater. Sci. Forum*, 383 (2002) 143.
21. R.A. Andrievski, *Mater. Trans.* 42, (2001) 1471.
22. Th. Lampke, A. Leopold, D. Dietrich, G. Alisch, B. Wielage, *Surf. Coat. Technol.*, 201 (2006) 3510.
23. H. Fong, D.H. Reneker In: D.R. Salem, Editor, Structure formation in polymeric fibers, Munich, Hanser, (2001) p. 225 - 246.
24. G.M. Whitesides, B. Grzybowski, *Science*, 295 (2002) 2418.

25. P.X. Ma, R. Zhang, *J. Biomed. Mat. Res.*, 46 (1999) 60.
26. T. Ondarcuhu, C. Joachim, *Europhys. Lett.*, 42 (1998) 215.
27. L. Feng, S. Li, H. Li, J. Zhai, Y. Song, L. Jiang, et al., *Angew Chem. Int. Ed.*, 41 (2002) 1221.
28. S.C. Tjong, Haydn Chen, *Materials Science and Engineering R*, 45 (2004) 1-88.
29. L. Maya, W.R. Allen, *J. Vac. Sci. Technol.*, B 13 (2) (1995) 361.
30. S. Veprek, A.S. Argon, *Surf. Coat. Technol.*, 146–147 (2001) 175.
31. V. Provenzano, R.L. Holtz, *Mater. Sci. Eng. A*, 204 (1995) 125.
32. R.A. Andrievski, A.M. Gleze, *Scripta Mater.*, 44 (2001) 1621.
33. El-Sayed M. Sherif, M. Es-saheb, A.A. Elzatahry, El-Refaie kenawy, A.S. Alkaraki, *Int. J. Electrochem. Sci.*, 7 (2012) 6154.
34. M. Es-saheb, A.A. Elzatahry, El-Sayed M. Sherif, A.S. Alkaraki, El-Refaie kenawy, *Int. J. Electrochem. Sci.*, 7 (2012) 5962.
35. El-Sayed M. Sherif, A.A. Almajid, F.H. Latif, H. Junaedi, *Int. J. Electrochem. Sci.*, 6 (2011) 1085
36. El-Sayed M. Sherif, *Int. J. Electrochem. Sci.* 6 (2011) 1479.
37. El-Sayed M. Sherif, *J. Mater. Eng. Performance*, 19 (2010) 873.
38. El-Sayed M. Sherif, A.H. Ahmed, Synthesis and Reactivity in Inorganic, *Metal-Organic, and Nano-Metal Chemistry*, 40 (2010) 365.
39. El-Sayed M. Sherif, R.M. Erasmus, J.D. Comins, *J. Appl. Electrochem.*, 39 (2009) 83.
40. El-Sayed M. Sherif, A.A. Almajid, *J. Appl. Electrochem.*, 40 (2010) 1555.
41. A.El Warraky, H.A. El Shayeb, E.M. Sherif, *Anti-Corros. Methods Mater.*, 51 (2004) 52.
42. Khalil A. Khalil, El-Sayed M. Sherif, A.A. Almajid, *Int. J. Electrochem. Sci.*, 6 (2011) 6184.
43. R. Karpagavalli, S. Rajeswari, *Anti-Corros. Methods Mater.*, 45 (1998) 333.
44. El-Sayed M. Sherif, *J. Solid State Electrochem.*, 16 (2012) 891.
45. El-Sayed M. Sherif, J. H. Potgieter, J. D. Comins, L. Cornish, P. A. Olubambi, C. N. Machio, *J. Appl. Electrochem.*, 39 (2009) 1385.
46. El-Sayed M. Sherif, *Int. J. Electrochem. Sci.*, 6 (2011) 3077.
47. El-Sayed M. Sherif, *Mater. Chem. Phys.*, 129 (2011) 961.
48. El-Sayed M. Sherif, A. A. Almajid, A. K. Bairamov, Eissa Al-Zahrani, *Int. J. Electrochem. Sci.*, 6 (2011) 5430.
49. El-Sayed M. Sherif, A.A. Almajid, *Int. J. Electrochem. Sci.*, 6 (2011) 2131.
50. H. Ma, S. Chen, L. Niu, S. Zhao, S. Li, D. Li, *J. Appl. Electrochem.*, 32 (2002) 65.
51. F. Mansfeld, S. Lin, S. Kim, H. Shih, *Corros. Sci.*, 27 (1987) 997.